Sci. Rep. Kanazawa Univ. **ARTICLES**
Vol. 68, pp. 153-170, 2025

Molecular Dynamics Simulation and Binding Free Energy Analysis of BAK1 and BRI1 Receptors Interacting with ANP Ligand in *Arabidopsis thaliana*

Lince MERIKO*, Kazutomo KAWAGUCHI and Hidemi NAGAO

Graduate School of Natural Science and Technology, Kanazawa University
Kanazawa, 920-1192, Japan

(Received June 27, 2025 and accepted in revised form August 18, 2025)

Abstract Brassinosteroids (BRs) are hormones that regulate various physiological processes essential for the normal growth and development of plants, including *Arabidopsis thaliana*. Based on the functional roles of the receptor kinases BAK1 and BRI1 in BR signaling, this study investigated the interactions between BAK1 and BRI1 proteins and the ANP (Phosphoaminophosphate Acid-Adenylate Ester) ligand using molecular docking, molecular dynamics (MD) simulations, and free energy calculations. Molecular docking demonstrated that the ANP ligand can effectively bind to the active sites of BAK1 and BRI1, potentially enhancing their activity and thus supporting plant growth and development. MD simulations were performed for 250 ns to evaluate the dynamic behavior and stability of these complexes. Analysis of the Root Mean Square Deviation (RMSD), Solvent Accessible Surface Area (SASA), Radius of Gyration (Rg), and hydrogen bonding indicated that the BAK1-ANP and BRI1-ANP complexes reached equilibrium and maintained structural stability throughout the simulation period. Furthermore, binding free energy calculations were performed using MM/GBSA (Molecular Mechanics/Generalized Born Surface Area) and MM/PBSA (Molecular Mechanics/Poisson-Boltzmann Surface Area) methods. The results showed negative binding free energy values for both complexes, indicating a favorable and spontaneous binding interaction between the ANP ligand and the receptor protein. This finding is consistent with the molecular docking results and further confirms that ANP can interact stably with BAK1 and BRI1, potentially modulating the BR signaling pathway in *Arabidopsis thaliana*.

Keywords. *Arabidopsis thaliana*, protein, ligand, docking, simulation

1. Introduction

Brassinosteroids (BR) are a class of polyhydroxysteroids known as essential phytohormones that regulate a variety of developmental and physiological processes in plants, including cell elongation, vascular differentiation, seed germination, abiotic and biotic stress responses [1,2]. BR perception and signal transduction are initiated at the plasma membrane through a receptor complex consisting primarily of Brassinosteroid Insensitive 1 (BRI1), Leucine-Rich Repeat Receptor-Like Kinase (LRR-RLK), and its co-receptor BRI1-Associated Receptor Kinase 1 (BAK1) [3]. Upon BR binding, BRI1 undergoes a conformational shift that facilitates heterodimerization with BAK1, triggering a concerted transphosphorylation event that activates downstream signaling cascades [4,5].

BAK1, originally identified in *Arabidopsis thaliana*, not only functions in BR signaling but also plays a role in innate immunity and other hormonal pathways [6]. The dynamic interaction between BRI1 and BAK1 is critical for the amplification and specificity of BR signal transduction. Structural and functional studies have shown that the formation of the BRI1-BAK1 complex is critical for kinase activation and subsequent transcription

* *Corresponding author* E-mail: lince@wriron1.s.kanazawa-u.ac.jp

factor phosphorylation that modulates gene expression [7]. Adenylic Acid Phosphoaminophosphate (ANP) esters are stable synthetic molecules that function as mimics of naturally occurring phosphate-containing compounds. As phosphomimetic ligands, ANP replicate the structure of phosphate groups commonly found in biological ligands. These compounds are widely used in the analysis of ATP-binding domains and support the study of protein kinase activation, including BAK1 and BRI1. Furthermore, ANP facilitates a deeper understanding of ligand recognition mechanisms in the brassinosteroid signaling pathway [8,9].

In molecular dynamics (MD) simulations and docking experiments, ANP was found to bind stably within the active sites of BRI1 and BAK1, forming favorable hydrogen bonds and van der Waals interactions. These interactions can either enhance or inhibit the formation of the BRI1-BAK1 complex, depending on the orientation of the binding site and the conformational changes. Consequently, ANP has potential as a chemical probe to modulate receptor activation and study the BR signaling mechanism in more detail. Furthermore, it provides a model to understand how non-natural ligands can regulate receptor-like kinase activity and downstream gene expression in plant cells.

Recent advances in computational biology, particularly molecular docking and MD simulations, have offered powerful tools to explore protein-ligand interactions at atomic resolution. These methods allow prediction of binding conformation, energetics, and dynamic behavior of protein-ligand complexes under near-physiological conditions [10,11]. Such approaches have been widely used in studying the interactions of BR receptors with natural or synthetic ligands, providing insights into the mechanisms of receptor activation and ligand specificity [12].

The purpose of this study was to investigate the molecular basis of ligand recognition and receptor activation in BR signaling by focusing on the interaction between the coreceptor BAK1 and the primary BR receptor BRI1 with ANP ligand. By analyzing the binding dynamics and interaction profiles, this study is expected to elucidate the molecular basis of BR receptor activation and provide computational insights into the ligand recognition mechanism that supports BR signaling in *Arabidopsis thaliana.*

2. Computational Methods

2.1. Preparation of Protein and Ligand

The crystal structure of the BAK1 (PDB ID: 3UIM resolution 2.20Å) [12] and BRI1 (PDB ID: 4OH4, resolution: 2.25 Å) [12] was retrieved from the Research Collaboratory for Structural Bioinformatics (RCSB) Protein Data Bank (https://www.rcsb.org/) in PDB format (Figure 1) [12]. The structure was then opened and prepared using AutoDockTools 4.2 prior to molecular docking simulations [13]. This step involved removing water molecules, adding polar hydrogen atoms, and assigning charges, ensuring that the protein structure was suitable for docking studies. The ligand was then converted to the appropriate file format (pdbqt) using AutoDockTools to prepare it for docking. The ligand atoms were assigned proper charges, and rotatable bonds were set to allow flexibility during the docking procedure.

This was followed by the removal of water molecules and heteroatoms, along with the addition of polar hydrogens to the target protein. Subsequently, Kollman charges were assigned to the protein, and the prepared structure was saved in pdbqt format for docking simulations. The process of preparing the protein structure ensures that it is compatible with docking software, allowing for accurate ligand binding predictions.

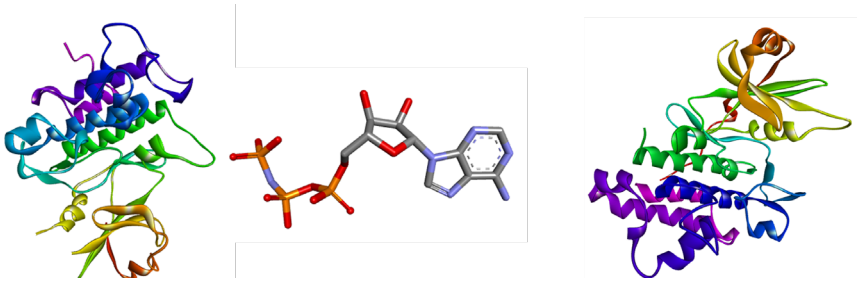

Figure 1. Crystal structure of BAK1 and BRI1 (PDB ID: 3UIM and 4OH4) and ANP ligand (https://www.rcsb.org/).

2.2. Molecular Docking Study

To investigate the binding interactions between the selected ligand and the protein target (BAK1 and BRI1), molecular docking studies were conducted using both AutoDock 4.2 and AutoDock Vina [14,16]. In this study, blind docking was employed to allow an unbiased search across the entire protein surface. This approach is especially useful when the active binding sites are unknown or to validate potential alternative binding regions.

AutoDock 4.2 applies to a combination of Monte Carlo simulated annealing, evolutionary algorithms, and the Lamarckian genetic algorithm to explore ligand conformations while maintaining the target protein as a rigid structure [17]. Grid maps required for docking were generated using AutoGrid, with the grid box dimensions set to 24 × 24 × 36 Å and a spacing of 1 Å to fully cover the entire protein structure (grid center: X = 10.676, Y = 1.954, Z = –14.824). The number of genetic algorithm (GA) runs was set to 100 with a population size of 300, while other GA parameters were kept at their default settings.

Both docking tools utilize an empirical scoring function to estimate binding affinities, where more negative binding energy values represent stronger predicted interactions. Ligand-protein complexes with the most favorable (i.e., lowest) binding energy values were prioritized for further molecular dynamics simulations and binding free energy calculations [18,19].

2.3. Visualization of Protein-Ligand Interactions

To gain a deeper understanding of the molecular interactions between the ligands and the target proteins (BAK1 and BRI1), the resulting docked complexes were analyzed using LigPlot+ (version 2.3.1). LigPlot+ is a widely used tool for generating two-dimensional (2D) schematic diagrams of ligand-protein interactions [20]. The software identifies and displays key intermolecular interactions, specifically hydrogen bonds and hydrophobic contacts, between the ligand functional groups and the amino acid residues at the binding site. The program operates through a graphical user interface written in Java and is highly effective in simplifying complex structural data into interpretable 2D diagrams.

In addition, two-dimensional (2D) and three-dimensional (3D) analyses and visualizations of the protein-ligand complexes were performed using BIOVIA Discovery Studio 2025 [21]. This combination of 2D and 3D visualization provides a comprehensive view of the molecular recognition patterns involved in ligand binding.

2.4. Molecular Dynamics (MD) Simulation

MD simulations were carried out to investigate the dynamic stability and binding behavior of the ligand protein complexes involving BAK1 and BRI1 proteins. Simulations were performed using the GROMACS 2020 package on a Linux system running Ubuntu 20.04.5 LTS. This step aimed to validate the docking results and to provide a more detailed understanding of ligand stability within the active sites under physiological conditions [22,23].

From the molecular docking results, the top scoring ligand was selected for further simulation in complex with both BAK1 and BRI1. Each system was simulated for 250 ns. Protein topology files were generated using the CHARMM36 force field [24], while the ligand topology was prepared using the CGenFF server (GEnFF) via the GlycoBioChem (Gallon) automated topology server [25].

The protein-ligand complexes were solvated in a triclinic periodic box filled with TIP3P water molecules (BAK1-ANP complex, the water content ranged from 719 to 23.301 molecules and the BRI1-ANP system contained between 12.671 and 18.115 molecules) to simulate a realistic biological environment. To ensure charge neutrality, Na^+ or Cl^- ions were added. After energy minimization and equilibration (NVT and NPT), a 250 ns production run was executed. Throughout the simulations, key structural and dynamic parameters were evaluated, including root mean square deviation (RMSD), Solvent Accessible Surface Area (SASA), radius of gyration (Rg), and the number of hydrogen bonds formed during the trajectory. The GROMACS built-in tools gmx rms, gmx gyrate, and gmx hbond were employed for these analyses.

2.5. Binding Free Energy Calculation

Binding free energy estimation was performed using the MM/GBSA (Molecular Mechanics/Generalized Born Surface Area) and MM/PBSA (Molecular Mechanics/Poisson-Boltzmann Surface Area) methods, implemented with the gmx_MM/PBSA tool (version 1.6.0) [26]. Calculations were conducted for the last 10 ns of the molecular dynamic's trajectory, based on the following equation [27,28]:

$$\Delta G_{bind} = \{G_{complex}\} - \{G_{receptor}\} - \{G_{ligand}\} = \Delta H - T\Delta S = \Delta E_{MM} + \Delta G_{sol} - T\Delta S,$$
$$\Delta E_{MM} = (\Delta E_{bond} + \Delta E_{angle} + \Delta E_{dihedral}) + \Delta E_{ele} + \Delta E_{vdW},$$
$$\Delta G_{sol} = \Delta G_{GB} + \Delta G_{non\text{-}polar.}$$

The binding free energy (ΔG_{bind}) was estimated as the difference in Gibbs free energy between the protein-ligand complex ($G_{complex}$), the unbound receptor proteins ($G_{receptor,\ BAK1\ and\ BRI1}$), and the unbound ligand ($G_{ligand,\ ANP}$), following the equation $\Delta G_{bind} = \Delta H - T\Delta S$. Here, ΔH represents the binding enthalpy, while $-T\Delta S$ accounts for the entropic contribution due to conformational changes upon ligand binding. The enthalpy term (ΔH) includes the molecular mechanical energy in the gas phase (ΔE_{MM}) and the solvation free energy (ΔG_{sol}). The ΔE_{MM} component consists of bonded interactions (bond, angle, and dihedral terms), as well as non-bonded interactions, including electrostatic (ΔE_{ele}) and van der Waals (ΔE_{vdW}) energies. The solvation free energy (ΔG_{sol}) is the sum of the polar contribution, calculated using the Generalized Born (GB) and Poisson Boltzmann (PB) models, and the non-polar component (ΔE_{surf}), which is estimated based on the solvent-accessible surface area (SASA). To identify key molecular determinants of binding, the per-residue free energy decomposition was performed, allowing the evaluation of individual amino acid and ligand contributions to the total interaction energy.

3. Results and Discussion

3.1. Molecular Docking Analysis

Molecular docking simulations were conducted to evaluate the binding affinities and interaction profiles of selected ligands with the BAK1 and BRI1 receptor proteins. The goal was to identify the most promising ligand candidates based on their docking performance and potential binding modes within the target active sites. The calculated binding energies show that ANP binds more strongly to BAK1 (ΔG = –3.99 kcal/mol) than to BRI1 (ΔG = –2.16 kcal/mol). This difference of 1.83 kcal/mol corresponds to a significant change in binding affinity, where each 1.36 kcal/mol change typically represents a tenfold difference in binding strength at 298K. The lowest binding energy conformations for the complexes, –4.64 kcal/mol for BAK1 and –3.38 kcal/mol for BRI1, further suggest that BAK1 provides a more favorable environment for ANP binding (Table 1).

Table 1. Molecular docking results of the ANP ligand with BAK1 and BRI1 proteins showing the lowest and mean binding energies.

Protein	Ligand	Lowest Binding Energy (kcal/mol)	Mean Binding Energy (kcal/mol)
BAK1	ANP	–4.64	–3.99
BRI1	ANP	–3.38	–2.16

With the aim of achieving comprehensive sampling and docking reliability, an initial screening was conducted using AutoDock 4.2, which employs a combination of Monte Carlo simulated annealing, genetic algorithms, and the Lamarckian genetic algorithm to explore ligand conformations [17]. Identical docking conditions were subsequently applied using AutoDock Vina, which integrates a sophisticated scoring function and a gradient-based conformational search algorithm, optimized for both accuracy and computational efficiency [29].

To better understand the molecular basis of ligand recognition, 2D interaction profiles of each protein-ligand complex were generated using LigPlot+ [30]. Table 2 and Figure 3 show the analysis, which allowed the identification of critical amino acid residues involved in hydrogen bonding, hydrophobic interactions in the binding pocket, and the observed molecular interactions between the ANP ligand and the BAK1 and BRI1 receptors, using LigPlot+ analysis. These interactions provide insight into the binding specificity and potential activation mechanisms of the two receptors in BR signaling.

Both receptors show attractive charge interactions with positively charged lysine residues Lys418 and Lys317 in BAK1, and Lys911 in BRI1. These residues are likely to engage with the negatively charged phosphate group of the ANP molecule. Electrostatic interactions, especially those involving lysines and arginine, are known to contribute significantly to the affinity and orientation of ligands in the kinase binding pocket [31].

Hydrogen bonding is an important determinant of binding stability and specificity. BRI1 forms a more extensive hydrogen bond network (6 residues), including Ser891, Gly895, and Ser1026, compared to only Met366 and Pro364 in BAK1. These conventional hydrogen bonds aid ligand binding and may contribute to the higher binding free energy observed in the BRI1-ANP complex, consistent with BRI1's role as a primary receptor [32].

Table 2. Key molecular interactions between ANP ligand and BAK1 and BRI1 proteins as identified using LigPlot+.

No	Type of Interaction	BAK1 Residues	BRI1 Residues
1	Attractive Charge	Lys418	Lys911
2	Salt Bridge	Lys317	-
2	Conventional H-bond	Met366, Pro364	Met959, Ser891, Gly895, Phe894, Gly893, Ser1026
3	Carbon H-bond	Leu295	Phe958
4	Pi-Donor Hydrogen Bond	-	Asn1014
5	Pi-Pi Stacked	Tyr365	-
6	Pi-Sigma	Leu423	Leu1016
7	Pi-Alkyl	Ala315, Val303	Ala909
8	Van der Waals	Arg297, Ser370, Gly296, Gly298, Gly299, Gly269, Tyr363, Leu347, Asn421, Asp434, Ala420	Val940, Tyr956, Glu957, Gly892, Val897, Asp896, Lys1011, Asp1027, Gly962, Gly890, Ile889

BAK1 exhibits Pi-Pi stacking interactions with Tyr365, whereas BRI1 does not exhibit such aromatic stacking. However, both receptors exhibit Pi-Alkyl and Pi-Sigma interactions that stabilize the ligand through hydrophobic contacts, involving residues such as Ala315, Val303 (BAK1) and Ala909 (BRI1). These nonpolar interactions are important for stabilizing ATP analogs in the kinase domain. Van der Waals interactions are the most abundant category, with both receptors exhibiting extensive contact surfaces. BAK1 involves residues such as Gly296-Gly299 and Tyr363, while BRI1 involves Val940, Asp896, and others. These extensive interactions indicate a highly compatible ligand-receptor interface that supports ligand activation [33].

Figures 2 and 3 show a three-dimensional (3D) and two-dimensional (2D) representations of hydrogen bonds formed between the ANP ligand and key residues of the BAK1 and BRI1 proteins. These findings provide a structural basis for selecting ligands with optimal binding properties for further validation through molecular dynamics simulations and free energy calculations.

Based on Table 2 and Figure 2, BRI1 is more variable in interacting with ANP compared to BAK1, especially in hydrogen bonds and Van der Waals contacts. This supports the hypothesis that BRI1 functions as a primary receptor in BR signaling, while BAK1 acts as a coreceptor, contributing to signal stabilization rather than direct recognition [34,35].

Hydrogen bonds play a crucial role in stabilizing protein-ligand complexes and are often key determinants of binding specificity and affinity. In protein kinases such as BAK1 and BRI1, the presence of conserved polar residues in the ATP-binding domain facilitates hydrogen bond formation with phosphate-mimicking ligands such as ANP. This interaction can enhance ligand anchorage and contribute to the conformational changes required for receptor activation. Previous studies have shown that stable hydrogen bonding patterns correlate with higher binding affinity and functional ligand efficacy at receptor kinases [36,37].

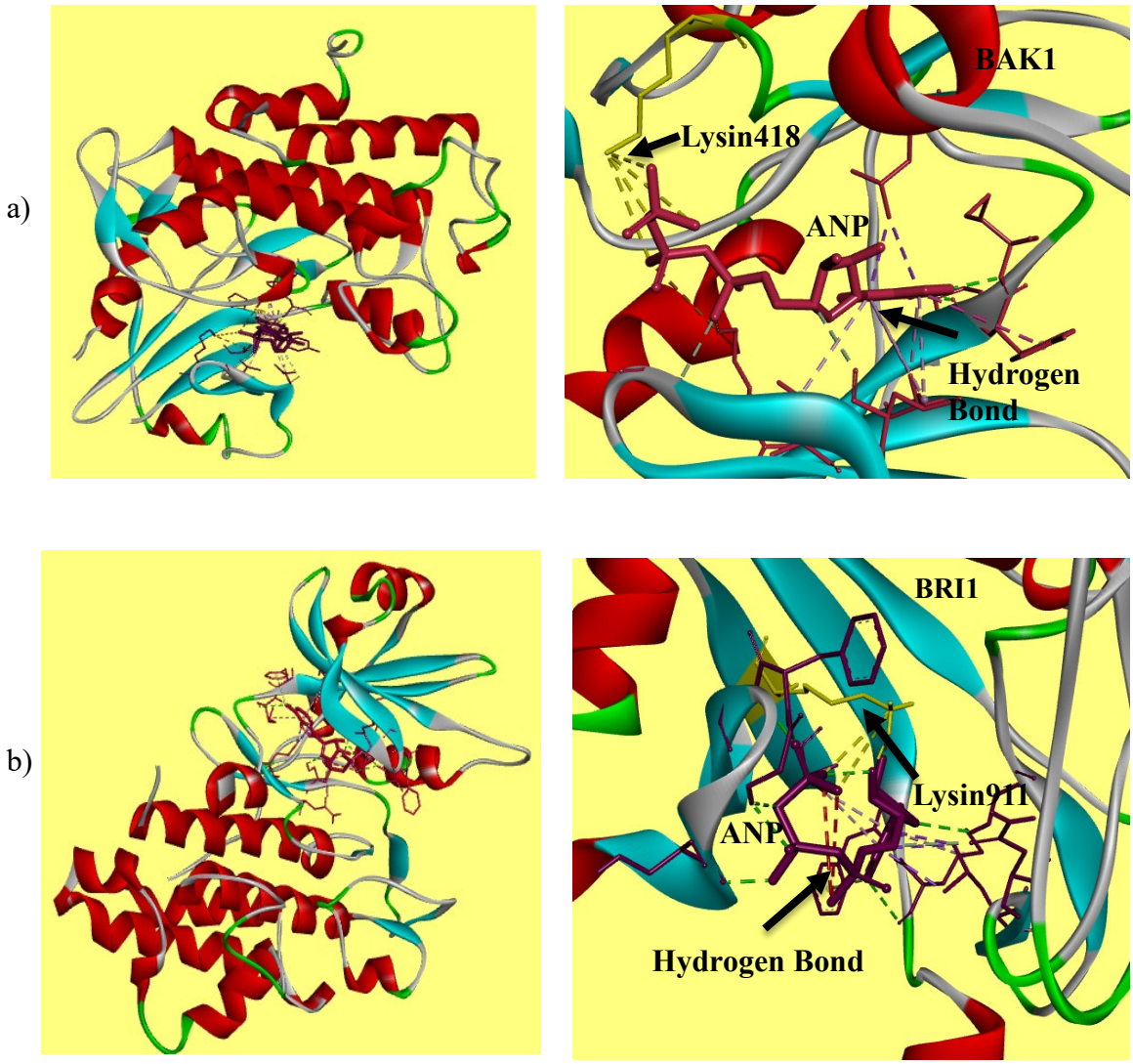

Figure 2. Three-dimensional view of ANP Ligand interacting with protein, a. ANP ligand interacting with BAK1, b. ANP ligand interacting with BRI1.

Furthermore, molecular dynamics simulation analyses have shown that persistent hydrogen bonding contributes to decreased ligand mobility and increased complex lifetime, particularly under physiological conditions. In the case of the BAK-ANP and BRI-ANP complexes, the observed hydrogen bond networks are highly informative. This suggests that ANP can stably interact with both receptor components, potentially mimicking natural hormonal triggers and facilitating the proper assembly of signaling complexes. This information is crucial not only for understanding the molecular basis of receptor activation but also for guiding the rational design and optimization of synthetic ligands aimed at modulating brassinosteroid signaling. By targeting key hydrogen bond-forming residues, future ligand design strategies could improve binding efficiency and selectivity, paving the way for novel agrochemical or biotechnological applications.

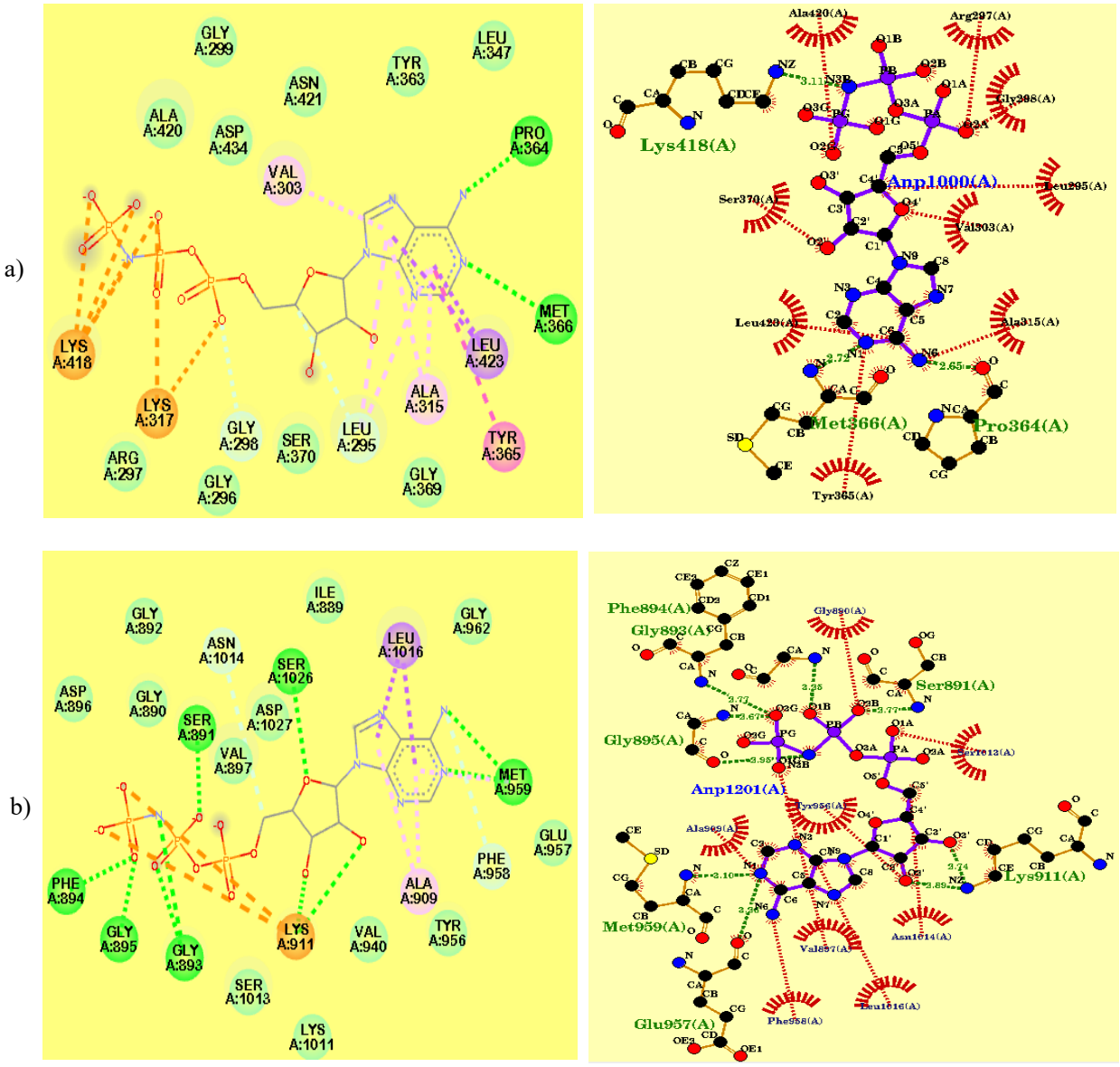

Figure 3. Two-dimensional representation of ligands interacting with amino acid residues of the proteins. a) Interaction of the ANP ligand with the BAK1 protein, b) Interaction of the ANP ligand with the BRI1 protein (the red dashed lines indicate hydrophobic interactions, while the green dashed lines indicate hydrogen bonds involved in these interactions).

3.2. Molecular Dynamic Simulation of ANP Ligand and Proteins

BAK1 and BRI1 function cooperatively in brassinosteroid signaling in *Arabidopsis thaliana*, where their kinase domains tightly regulate ligand perception and downstream signaling. ANP's strong binding affinity for the BAK1 and BRI1 receptors suggests potential modulatory and competitive mechanisms. Specifically, ANP can interfere with the binding of endogenous ligands, thereby disrupting normal receptor signaling, while mimicking their function in modulating downstream responses. This observation is in line with previous studies, which demonstrate that kinase-ligand interactions play a significant role in shaping signaling outcomes [38,39]. ANP, being a nucleotide derivative, may resemble ATP analogs, which can either activate or inhibit kinase function depending on

the context of the binding. These findings are particularly valuable for designing small molecule modulators targeting the BRI1 and BAK1 complex, which could have applications in agriculture or biotechnology.

Building on the molecular docking results, MD simulations of the BAK1-ANP and BRI1-ANP complexes were performed. A 250 ns MD run was conducted for both complexes, and the resulting trajectories were analyzed to evaluate various structural properties of the protein-ligand complexes, including the root mean square deviation (RMSD), Radius of gyration (Rg), Solvent Accessible Surface Area (SASA), and hydrogen bonds over time. The RMSD provides insight into the structural stability of the ligand-protein complex during the simulation. An RMSD value of less than 0.4 nm (4 Å) is generally considered acceptable, indicating minimal variation and suggesting that the complex remains stable [40].

RMSD Analysis

Figure 4 shows the combined backbone RMSD graphs for the BAK1 and BRI1 protein-ligand complexes. In this study, the RMSD of the BAK1-ANP complex remained low and stable between 0.20-0.25 nm throughout the 250 ns simulation, showing that the structure stayed compact and well folded. This suggests strong interactions between the protein and ligand. On the other hand, the BRI1-ANP complex had higher RMSD values, fluctuating between 0.25-0.35 nm, with a gradual increase over time.

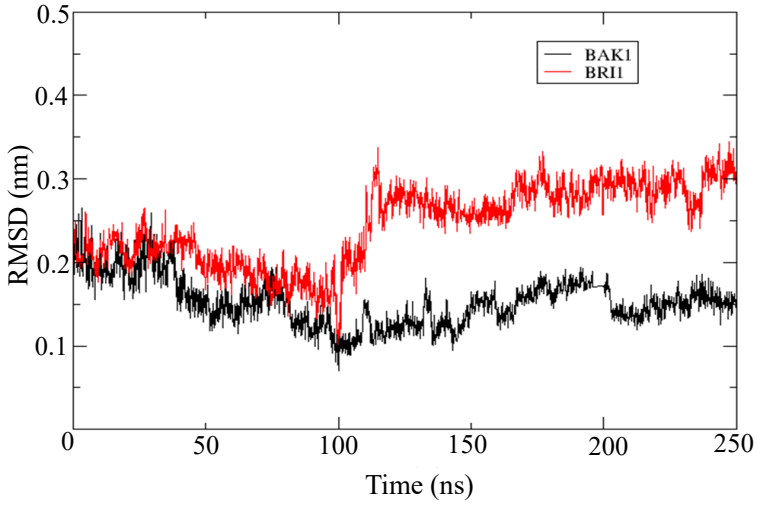

Figure 4. RMSD plots of BAK1 and BRI1 protein complex for 250ns.

This pattern suggests a higher degree of flexibility or potential structural rearrangements occurring within the protein during ligand binding. Such conformational plasticity often reflects the dynamic nature of protein-ligand interactions, particularly in signaling receptors where structural adaptation is crucial for functional activation. This observation aligns with previous studies showing that BAK1 functions primarily as a structural stabilizer within the receptor complex, maintaining the integrity of the signaling unit. In contrast, BRI1 exhibits greater flexibility, allowing it to undergo the necessary conformational changes to accommodate ligand binding. This adaptive behavior of BRI1 is crucial for the initiation and propagation of downstream signaling events, as it facilitates proper alignment and interaction with the ligand and the BAK1 co-receptor. These

differential roles between BRI1 and BAK1 have been further supported by molecular dynamics simulations, which revealed that the kinase domain of BRI1 exhibits higher conformational variability, while BAK1 maintains a more rigid and stable active conformation [41].

SASA Analysis

SASA measures how much of the protein surface is exposed to the surrounding water. It reflects the protein's compactness and conformational changes. In our simulations, the BAK1-ligand complex had an average SASA of 163 nm², which remained relatively constant, suggesting a stable and folded protein structure with minimal exposure to the solvent. In contrast, the BRI1-ligand complex had higher SASA values, around 168-170 nm², suggesting that it was more exposed to the solvent and possibly more flexible (Figure 5).

This difference may be due to larger and more dynamic extracellular regions in BRI1, which have been reported in earlier structural modeling studies. These flexible extracellular domains allow BRI1 to adopt multiple conformations, facilitating diverse ligand recognition and enabling adaptive binding mechanisms. Such structural versatility is crucial for BRI1's role in perceiving various brassinosteroid signals and initiating downstream signaling cascades, distinguishing it functionally from the more rigid and stable architecture observed in BAK1 [42,43].

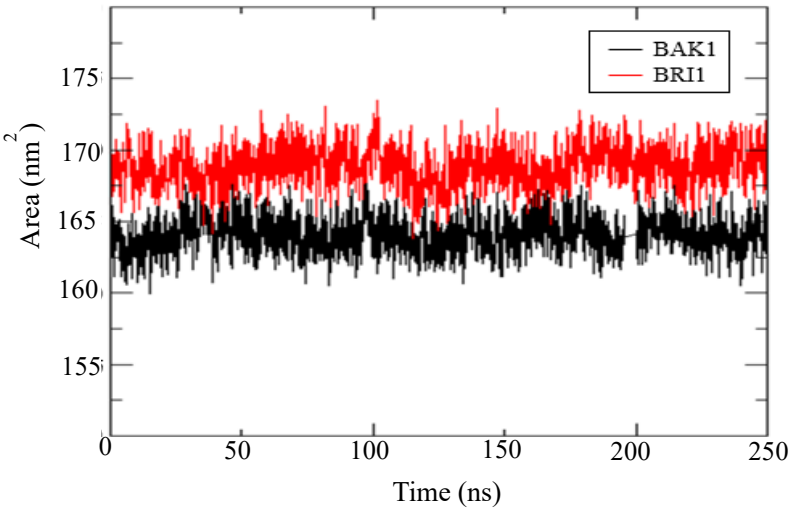

Figure 5. SASA plots of BAK1 and BRI1 protein complex for 250ns.

Rg Analysis

Rg values help us understand how tightly folded a protein is. It tells us about the overall compactness of the structure. The BAK1-ANP ligand had Rg values between 1.88-1.96 nm, showing a compact and stable fold. Meanwhile, the BRI1-ligand complex showed slightly higher Rg values of 1.96-2.02 nm, suggesting a more relaxed or flexible structure (Figure 6).

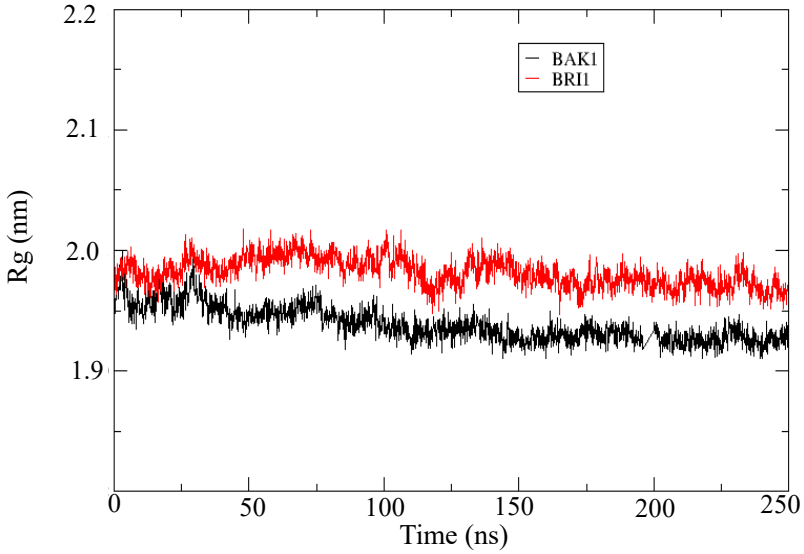

Figure 6. Rg plots of BAK1 and BRI1 protein complex for 250ns.

Snapshot images at 0 ns and 250 ns show conformational changes that reflect the results of the radius of gyration (Rg) analysis (Figure 7). At 0 ns, both the BAK1-ANP and BRI1-ANP complexes are still in their initial, relatively open states, reflecting structures that have not yet fully reached dynamic equilibrium. However, at 250 ns, the BAK1-ANP complex shows greater structural compaction compared to the initial frame. This is consistent with the decrease in Rg values observed during the simulation. This compaction indicates structural stability and a possible stronger interaction between BAK1 and the ANP ligand. Conversely, in the BRI1-ANP complex, the structural changes at 250 ns are not as pronounced as those seen in BAK1.

The BRI1 structure still shows open regions, which is consistent with the more fluctuating and relatively higher Rg values. This suggests that the interaction between BRI1 and the ANP ligand is likely weaker or less stable than that of BAK1. These results support that BAK1 plays a crucial role in stabilizing the complex with ANP, possibly related to its function as a co-receptor in brassinosteroid signaling in *Arabidopsis thaliana*. Furthermore, the greater compactness of the BAK1-ANP complex compared to BRI1-ANP indicates a better binding interface and possibly a stronger hydrogen bond network, consistent with the higher average number of hydrogen bonds in BAK1. This structural stability may enhance signal transduction efficiency and ligand retention, thus strengthening BAK1's role in facilitating receptor activation and maintaining complex integrity during signaling [45,46].

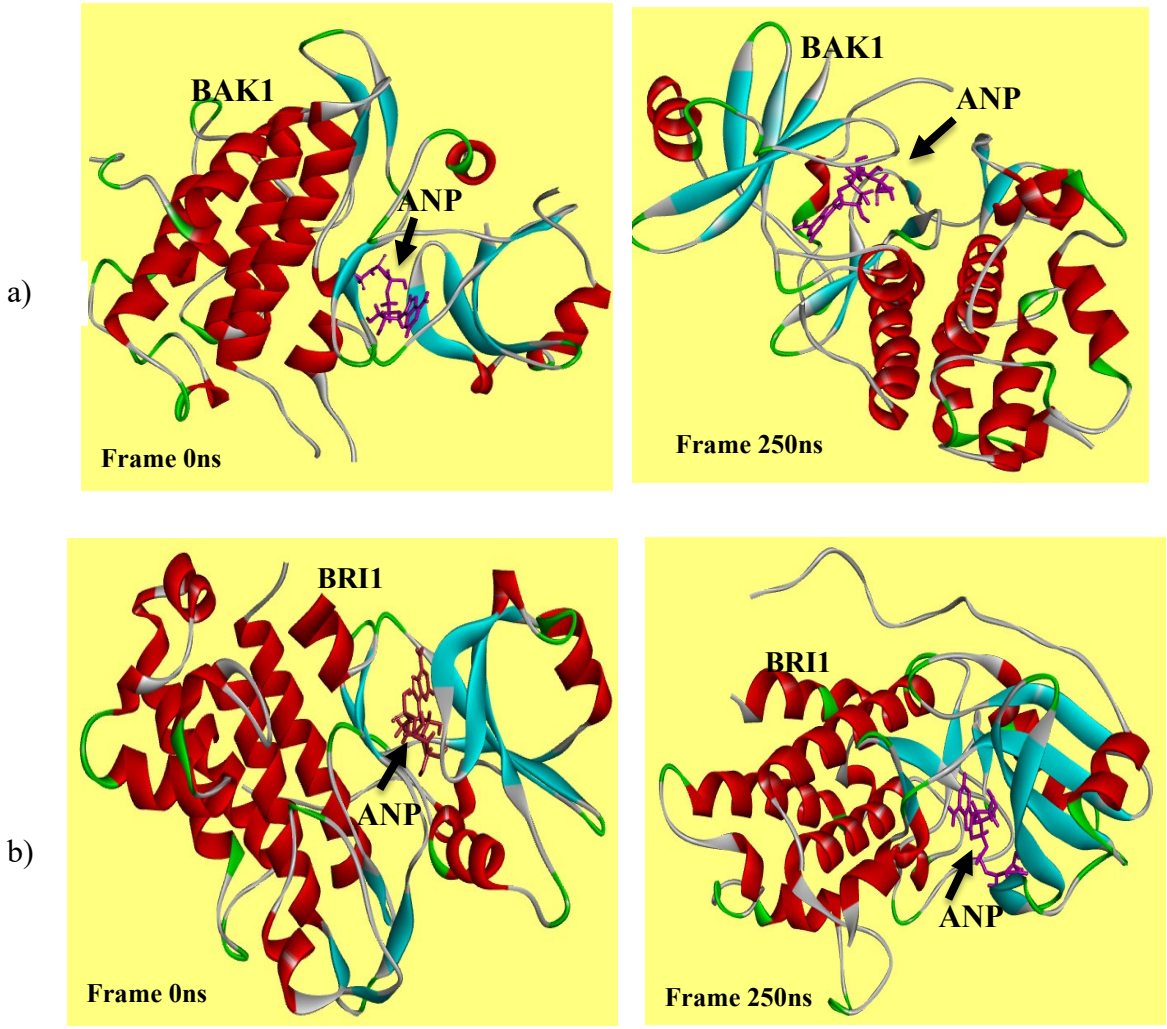

Figure 7. Structural snapshots at 0 ns and 250 ns of (a) the BAK1-ANP complex and (b) the BRI1-ANP complex.

Hydrogen Bond Analysis

Hydrogen bonds are essential for maintaining protein-ligand interactions. The number and stability of these bonds can indicate how strong the interaction is. In the BAK1-ligand complex, 3 to 6 hydrogen bonds were formed consistently over the 250 ns simulation. This suggests strong and sustained interactions between the ligand and the protein's binding site. The BRI1-ligand complex formed between 2 to 5 hydrogen bonds, but these interactions were more dynamic and variable, showing that the ligand interacts less consistently with BRI1 (Figure 8). This is supported by studies showing that more stable hydrogen bonds can enhance ligand-binding affinity, particularly in plant kinases. These findings highlight the importance of hydrogen bonding in determining ligand selectivity and receptor activation within the brassinosteroid signaling pathway. The stronger hydrogen bond network in BAK1 potentially facilitates more efficient receptor activation and maintains the stability of the signaling complex, thus strengthening its role as a co-receptor in brassinosteroid signaling in *Arabidopsis thaliana*. Conversely, the weaker and fluctuating hydrogen bonds

in BRI1 may contribute to more dynamic ligand binding behavior, which may ultimately affect ligand selectivity and downstream signaling efficiency [47].

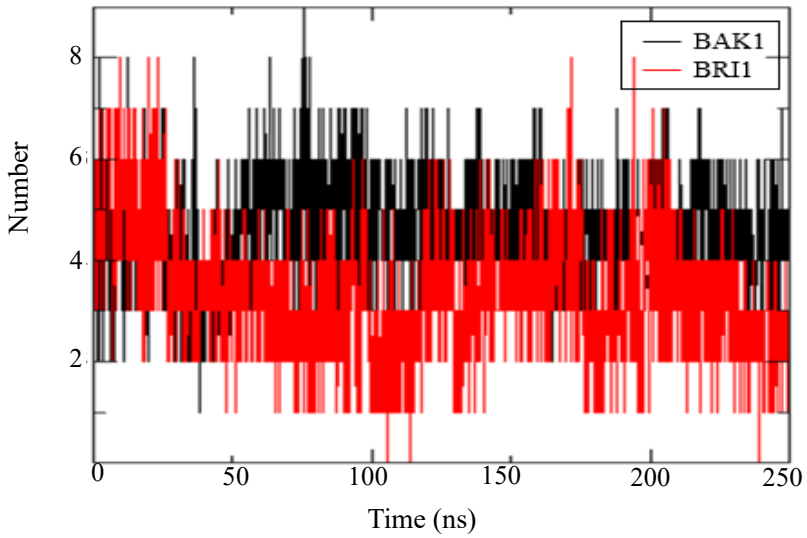

Figure 8. Number of hydrogen bonds of BAK1 protein complex for 250ns.

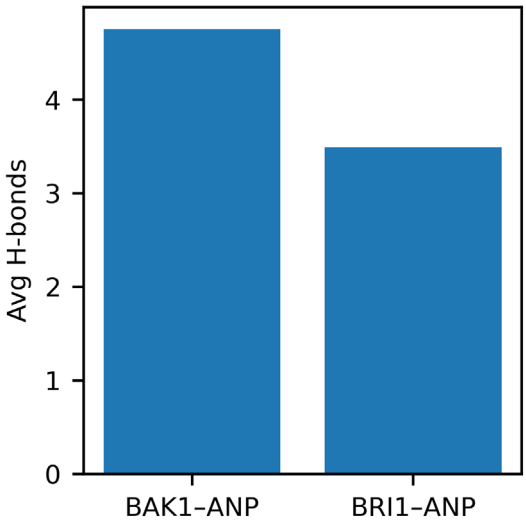

Figure 9. Average Hydrogen Bonds Between ANP with BAK1 and BRI1 Protein.

Hydrogen bonding is a crucial factor in maintaining the stability and specificity of protein-ligand interactions during molecular dynamics simulations. Quantitative analysis shows that the BAK1-ANP complex forms more hydrogen bonds than the BRI1-ANP complex. The average number of hydrogen bonds observed for BAK1-ANP was 4.8, while BRI1-ANP formed an average of only 3.5 hydrogen bonds (Figure 9). This difference indicates that ANP exhibits a stronger and more stable bond with BAK1 compared to BRI1. These results are consistent with previous studies showing that a higher number of hydrogen bonds contributes to increased affinity and thermodynamic stability in protein-ligand complexes [48,49]. In the context of brassinosteroid signaling in *Arabidopsis thaliana*, the

stronger interaction between ANP and BAK1 may play a crucial role in modulating the activity of the receptor complex during signal perception.

3.3. Binding Free Energy Analysis of BAK1 and BRI1 Complexes

The binding free energy values calculated using MM/GBSA and MM/PBSA methods as shown in Table 3, BAK1-ANP and BRI1-ANP complexes show negative binding free energy values, indicating a favorable and spontaneous interaction. MM/GBSA results show that the BRI1-ANP complex has a slightly stronger binding affinity (−28.93 kcal/mol) compared to the BAK1-ANP complex (−24.54 kcal/mol). MM/PBSA calculation of BAK1-ANP ligand produces better binding energy (−31.43 kcal/mol) than the BRI1-ANP complex (−20.65 kcal/mol).

Table 3. Binding free energy of Protein complex obtained using GB/PB calculation Delta (Complex-BAK1- ANP ligand, BRI1-ANP ligand).

ENERGY COMPONENT	BAK1-ANP (MM/GBSA) kcal/mol	BRI1-ANP (MM/GBSA) kcal/mol	BAK1-ANP (MM/PBSA) kcal/mol	BRI1-ANP (MM/PBSA) kcal/mol
ΔEvdW	–50.85	–48.99	–51.33	–49.51
ΔEele	–45.58	–77.32	–44.70	–77.11
ΔGGB or ΔEPB	78.45	104.15	69.18	110.41
ΔEsurf or ΔEnp	–6.55	–6.77	–4.57	–4.43
ΔGgas	–96.44	–126.31	–96.04	–126.63
ΔGsolv	71.90	97.38	64.61	105.98
ΔGtotal	**–24.54**	**–28.93**	**–31.43**	**–20.65**

Binding free energy analysis using MM/GBSA and MM/PBSA methods provided important insights into the thermodynamic stability of BAK1-ANP and BRI1-ANP complexes. As shown in Table 3, both complexes exhibit negative binding free energy values, indicating that the interaction between ANP ligand and BAK1, and BRI1 receptors is thermodynamically favorable and occur spontaneously under simulation conditions.
MM/GBSA results showed that the BRI1-ANP complex has a slightly stronger binding affinity with a binding energy of −28.93 kcal/mol compared to −24.54 kcal/mol for the BAK1-ANP complex. This suggests that under the generalized Born solvent model, ANP interacts more strongly with BRI1. This may reflect the role of BRI1 as a key receptor in the brassinosteroid (BR) signaling pathway, where ligand recognition often occurs first at BRI1 before BAK1 recruitment [50].

In contrast, MM/PBSA analysis showed a stronger binding interaction in the BAK1-ANP complex (−31.43 kcal/mol) than in the BRI1-ANP complex (−20.65 kcal/mol). The Poisson-Boltzmann solvent model often provides a more stringent electrostatic treatment compared to the GB model, and this result may indicate that BAK1 contributes significantly to the stabilization of the ANP ligand after binding in the ternary complex. This observation is consistent with the finding that BAK1 acts as a coreceptor and stabilizer in ligand-mediated receptor activation [51].

Differences between MM/GBSA and MM/PBSA binding free energy results for the BAK1-ANP and BRI1-ANP complexes are commonly reported. These differences arise from the distinct solvent models and energy calculation methods used by each approach.

MM/GBSA often overestimates van der Waals interactions due to its simplified solvation model, highlighting close contact between ANP and the protein surface. On the other hand, MM/PBSA is more sensitive to electrostatic and solvation effects, which play a critical role in ligand recognition by the ATP-binding domains of BAK1 and BRI1. By combining both methods, a more reliable understanding of the binding mechanisms and energetic contributions within these complexes can be achieved [52].

Overall, the data suggests that BAK1 and BRI1 have favorable interactions with ANP, but their relative contributions to ligand binding depend on the computational approach. These results may reflect dynamic ligand positioning within the receptor binding site and support the hypothesis that both receptors are involved in a cooperative ligand recognition mechanism in *Arabidopsis thaliana* [53].

4. Concluding Remark

This study investigated the binding mechanism of ANP ligand to the plant receptor proteins BAK1 and BRI1 through molecular simulations. Both receptors engage ANP through multiple non-covalent interactions. In 250 ns simulations, the complexes exhibited stability. The ANP-BAK1 complex maintained a more compact and stable conformation, while ANP-BRI1 exhibited stronger binding energy but increased flexibility and structural variability. These findings suggest that BAK1 provides a structurally stable binding environment for ANP, whereas BRI1 offers a more dynamic but energetically favorable interaction. The cooperative function of BAK1 and BRI1 likely plays a crucial role in plant hormone signaling. This work contributes to a deeper understanding of receptor-ligand dynamics and informs future efforts in designing modulators of the brassinosteroid signaling pathway.

Acknowledgments

This work was supported by JSPS KAKENHI Grant Numbers 23K03339 and 23K03338. Part of the computation was performed using Research Center for Computational Science, Okazaki, Japan (Project: 25-IMS-C041).

References

[1] Clouse, S.D., & Sasse, J.M. (1998). Brassinosteroids: Essential regulators of plant growth and development. Annual Review of Plant Physiology and Plant MolecularBiology,49(1),427–451. https://doi.org/10.1146/annurev.arplant.49.1.427.

[2] Nolan, T. M., et al. (2020). Brassinosteroids: Multidimensional regulators of plant growth, development, and stress responses. Plant Cell, 32(2), 295–318. https://doi.org/10.1105/tpc.19.00335.

[3] Wang, Z.Y., et al. (2001). Nuclear-localized BZR1 mediates brassinosteroid-induced growth and feedback suppression of brassinosteroid biosynthesis. Developmental Cell, 2(4), 505–513.

[4] Sun, Y., et al. (2013). Structural basis for flg22-induced activation of the Arabidopsis FLS2-BAK1 immune complex. Science, 342(6158), 624–628. https://doi.org/10.1126/science.1243825.

[5] Hohmann, U., et al. (2018). Mechanistic insights into the activation of plant membrane receptor kinases. Current Opinion in Plant Biology, 45, 1–6. https://doi.org/10.1016/j.pbi.2018.05.001.

[6] Chinchilla, D., et al. (2009). The Arabidopsis receptor kinase BAK1 functions in brassinosteroid signaling and basal defense. The Plant Cell, 21(7), 2147–2160.

https://doi.org/10.1105/tpc.108.064774.
[7] Li, J., & Chory, J. (1997). A putative leucine-rich repeat receptor kinase involved in brassinosteroid signal transduction. Cell, 90(5), 929–938.
[8] Powers, R., Mercier, K.A., & Copeland, J.C. (2001). Using NMR spectroscopy to study the structure and dynamics of protein–ligand interactions. Progress in Nuclear Magnetic Resonance Spectroscopy, 38(4), 373–396. https://doi.org/10.1016/S0079-6565(00)00041-0.
[9] Vidad, J.S., Wang, H., & Lin, M. (2022). Exploring phosphomimetic ligands in kinase signaling pathways: a computational approach. Journal of Molecular Modeling, 28, 112. https://doi.org/10.1007/s00894-022-05004-2.
[10] Pagadala, N.S., et al. (2017). Software for molecular docking: a review. Biophysical Reviews, 9, 91–102. https://doi.org/10.1007/s12551-016-0247-1.
[11] Durrant, J.D., & McCammon, J.A. (2011). Molecular dynamics simulations and drug discovery. BMC Biology, 9(1), 71. https://doi.org/10.1186/1741-7007-9-71.
[12] Tanaka, K., et al. (2019). Structural basis for brassinosteroid perception by BRI1. Nature, 474(7352), 472–476. https://doi.org/10.1038/nature10178.
[13] RCSB Protein Data Bank. (n.d.). Retrieved from https://www.rcsb.org/.
[14] Morris GM, Huey R, Lindstrom W, Sanner MF, Belew RK, Goodsell DS, Olson AJ. AutoDock4 and AutoDockTools4: automated docking with selective receptor f lexibility. J Comput Chem 2009 Dec;30(16):2785–91. https://doi.org/10.1002/jcc.21256.
[15] Berman HM, Westbrook J, Feng Z, Gilliland G, Bhat TN, Weissig H, Shindyalov IN, Bourne PE. The protein data bank. Nucleic Acids Res 2000 Jan 1;28(1):235–42. https://doi.org/10.1093/nar/28.1.235.
[16] Trott O, Olson AJ. AutoDock Vina: improving the speed and accuracy of docking with a new scoring function, efficient optimization, and multithreading. J Comput Chem 2010 Jan 30;31(2):455–61. https://doi.org/10.1002/jcc.21334.
[17] Morris, G. M., Huey, R., Lindstrom, W., Sanner, M. F., Belew, R. K., Goodsell, D. S., & Olson, A. J. (2009). AutoDock4 and AutoDockTools4: Automated docking with selective receptor flexibility. Journal of Computational Chemistry, 30(16), 2785–2791. https://doi.org/10.1002/jcc.21256.
[18] Trott, O., & Olson, A. J. (2010). AutoDock Vina: Improving the speed and accuracy of docking with a new scoring function, efficient optimization, and multithreading. Journal of Computational Chemistry, 31(2), 455–461. https://doi.org/10.1002/jcc.21334.
[19] Meng, X. Y., Zhang, H. X., Mezei, M., & Cui, M. (2011). Molecular docking: A powerful approach for structure-based drug discovery. Current Computer-Aided Drug Design, 7(2), 146–157. https://doi.org/10.2174/157340911795677602.
[20] Laskowski, R. A., & Swindells, M. B. (2011). LigPlot+: Multiple ligand–protein interaction diagrams for drug discovery. Journal of Chemical Information and Modeling, 51(10), 2778–2786. https://doi.org/10.1021/ci200227u.
[21] Schrödinger, LLC. (2015). The PyMOL Molecular Graphics System, Version 2.5. Available from: https://pymol.org
[22] Abraham, M. J., Murtola, T., Schulz, R., Páll, S., Smith, J. C., Hess, B., & Lindahl, E. (2015). GROMACS: High performance molecular simulations through multi-level parallelism from laptops to supercomputers. SoftwareX, 1–2, 19–25. https://doi.org/10.1016/j.softx.2015.06.001
[23] Lemkul, J. A. (2018). From Proteins to Perturbed Hamiltonians: A Suite of Tutorials for the GROMACS-2018 Molecular Simulation Package. https://doi.org/10.33011/tcb158

[24] Huang, J., & MacKerell, A. D. (2013). CHARMM36 all-atom additive protein force field: Validation based on comparison to NMR data. Journal of Computational Chemistry, 34(25), 2135–2145. https://doi.org/10.1002/jcc.23354.

[25] Vanommeslaeghe, K., & MacKerell, A. D. (2012). Automation of the CHARMM General Force Field (CGenFF) I: Bond perception and atom typing. Journal of Chemical Information and Modeling, 52(12), 3144–3154. https://doi.org/10.1021/ci300363c.

[26] Valdés-Tresanco, M. S., Valdés-Tresanco, M. E., Valiente, P. A., & Moreno, E. (2021). gmx_MMPBSA: A new tool to perform end-state free energy calculations with GROMACS. Journal of Chemical Theory and Computation, 17(10), 6281–6291. https://doi.org/10.1021/acs.jctc.1c00511.

[27] Homeyer, N., & Gohlke, H. (2012). Free energy calculations by the MM-PBSA method: Challenges, advances, and applications. Wiley Interdisciplinary Reviews: Computational Molecular Science, 2(1), 43–64. https://doi.org/10.1002/wcms.66.

[28] Genheden, S., & Ryde, U. (2015). The MM/PBSA and MM/GBSA methods to estimate ligand-binding affinities. Expert Opinion on Drug Discovery, 10(5), 449–461. https://doi.org/10.1517/17460441.2015.1032936.

[29] Trott, O., & Olson, A. J. (2010). AutoDock Vina: Improving the speed and accuracy of docking with a new scoring function, efficient optimization, and multithreading. Journal of Computational Chemistry, 31(2), 455–461. https://doi.org/10.1002/jcc.21334.

[30] Laskowski, R. A., & Swindells, M. B. (2011). LigPlot+: Multiple ligand–protein interaction diagrams for drug discovery. Journal of Chemical Information and Modeling, 51(10), 2778–2786. https://doi.org/10.1021/ci200227.

[31] Honig, B., & Nicholls, A. (1995). Classical electrostatics in biology and chemistry. Science, 268, 1144–1149. https://doi.org/10.1126/science.7761829

[32] Clackson, T., & Wells, J. A. (1995). A hot spot of binding energy in a hormone-receptor interface. Science, 267, 383–386. https://doi.org/10.1126/science.7529940

[33] Bissantz, C., Kuhn, B., & Stahl, M. (2010). A medicinal chemist's guide to molecular interactions. Journal of Medicinal Chemistry, 53(14), 5061–5084. https://doi.org/10.1021/jm100112j

[34] Santiago, J., et al. (2013). Mechanistic insight into a peptide hormone signaling complex mediating floral organ abscission. eLife, 2, e00564. https://doi.org/10.7554/eLife.00564

[35] Hohmann, U., et al. (2017). Mechanistic basis for the activation of plant membrane receptor kinases by SERK-family coreceptors. PNAS, 114(21), E4360–E4369. https://doi.org/10.1073/pnas.1704176114

[36] Liu, X.; Wang, Q.; Yang, G.; Tao, Y. Structure-Based Discovery of Kinase Inhibitors: Drug Binding and Conformational Dynamics. Biochim. Biophys. Acta Proteins Proteom. 2017, 1865, 58–66. https://doi.org/10.1016/j.bbapap.2016.10.004.

[37] Zhang, J.; Yang, P.; Wang, W.; Ma, W.; Zhang, S.; Li, Y. Phosphomimetic Ligands Reveal Conserved Features of Receptor Kinase Activation in Plants. Nat. Commun. 2021, 12, 1027. https://doi.org/10.1038/s41467-021-21207-0.

[38] Wang, X., et al. (2008). Brassinosteroid Signaling in Arabidopsis thaliana: Mechanisms of Action. Plant Cell, 20(2), 308–324. https://doi.org/10.1105/tpc.108.059106.

[39] Clouse, S. D. (2011). Brassinosteroid Signaling: From the Receptor to the Transcriptome. The Plant Cell, 23(4), 1200–1215. https://doi.org/10.1105/tpc.111.086564.
[40] Baker, N. A., et al. (2001). Electrostatics of Nucleic Acids: Insights into the Conformational Properties of DNA and RNA. Biophysical Journal, 80(1), 1–19. https://doi.org/10.1016/S0006-3495(01)76068-0.
[41] Taylor, M. G., He, Y., & Qi, Y. (2017). Structural and dynamic insights into the functional role of BAK1 in brassinosteroid signaling. PLoS ONE, 12(7), e0180909. https://doi.org/10.1371/journal.pone.0180909.
[42] Yang, Y., Sun, Y., Bao, Y., & Wang, W. (2023). Molecular basis for co-receptor function of BAK1 in receptor complexes. International Journal of Molecular Sciences, 24(2), 1174. https://doi.org/10.3390/ijms24021174.
[43] Hohmann, U., Lau, K., & Hothorn, M. (2017). The structural basis of ligand perception and signal activation by receptor kinases. Annual Review of Plant Biology, 68, 109–137. https://doi.org/10.1146/annurev-arplant-042916-040957.
[44] Cheng, Z., Li, J., & He, Z. (2020). Plant receptor-like kinases: From signaling to applications. Molecules, 25(23), 5390. https://doi.org/10.3390/molecules25235390.
[45] Santiago, J., et al. (2013). The crystal structure of the BRI1 ectodomain reveals a conserved brassinosteroid binding site. Nature, 474(7352), 472–476.
[46] Sun, Y., et al. (2013). Integration of brassinosteroid signal transduction with the transcription network for plant growth regulation. Developmental Cell, 19(5), 765–777.
[47] Ghosh, R., Chakraborty, P., & Ray, A. (2021). Investigating the role of hydrogen bonds in protein-ligand complexes using molecular dynamics. Journal of Molecular Graphics and Modelling, 106, 107926. https://doi.org/10.1016/j.jmgm.2021.107926.
[48] Wang, C., et al. (2019). Computational insights into protein–ligand interactions: The role of hydrogen bonding and hydrophobic contacts in stability. Journal of Molecular Graphics and Modelling, 92, 30–38. https://doi.org/10.1016/j.jmgm.2019.06.005.
[49] Rasheed, M., et al. (2022). Understanding the significance of hydrogen bonds in drug–protein interactions using molecular dynamics simulation. Scientific Reports, 12, 1443. https://doi.org/10.1038/s41598-022-05487-2.
[50] Belkhadir, Y., Jaillais, Y., Epple, P., Balsemão-Pires, E., Dangl, J. L., & Chory, J. (2012). Brassinosteroids modulate the efficiency of plant immune responses to microbe-associated molecular patterns. Proceedings of the National Academy of Sciences, 109(1), 297-302. https://doi.org/10.1073/pnas.1112840108.
[51] Clouse, S. D. (2011). Brassinosteroid signal transduction: from receptor kinase activation to transcriptional networks regulating plant development. The Plant Cell, 23(4), 1219–1230. https://doi.org/10.1105/tpc.111.084475.
[52] Genheden, S., & Ryde, U. (2015). The MM/PBSA and MM/GBSA methods to estimate ligand-binding affinities. Expert Opinion on Drug Discovery, 10(5), 449–461. https://doi.org/10.1517/17460441.2015.1032936.
[53] Sun, Y., Li, L., Macho, A. P., Han, Z., Hu, Z., Zipfel, C., & Chai, J. (2013). Structural basis for flg22-induced activation of the Arabidopsis FLS2-BAK1 immune complex. Science, 342(6158), 624–628. https://doi.org/10.1126/science.1243825.